



Open Research Online

The Open University's repository of research publications and other research outputs

The SMILE Soft X-ray Imager (SXI) CCD design and development

Journal Item

How to cite:

Soman, M.R.; Hall, D.J.; Holland, A.D.; Burgon, R.; Buggey, T.; Skottfelt, J.; Sembay, S.; Drumm, P.; Thornhill, J.; Read, A.; Sykes, J.; Walton, D.; Branduardi-Raymont, G.; Kennedy, T.; Raab, W.; Verhoeve, P.; Agnolon, D. and Woffinden, C. (2018). The SMILE Soft X-ray Imager (SXI) CCD design and development. *Journal of Instrumentation*, 13(1), article no. C01022.

For guidance on citations see [FAQs](#).

© 2018 IOP Publishing Ltd and Sissa Medialab

Version: Accepted Manuscript

Link(s) to article on publisher's website:

<http://dx.doi.org/doi:10.1088/1748-0221/13/01/C01022>

Copyright and Moral Rights for the articles on this site are retained by the individual authors and/or other copyright owners. For more information on Open Research Online's data [policy](#) on reuse of materials please consult the policies page.

oro.open.ac.uk

The SMILE Soft X-ray Imager (SXI) CCD design and development

M. R. Soman^{a,*}, D. J. Hall^a, A. D. Holland^a, R. Burgon^a, T. Buggey^a, J. Skottfelt^a, S. Sembay^b, P. Drumm^b, J. Thornhill^b, A. Read^b, J. Sykes^b, D. Walton^c, G. Branduardi-Raymont^c, T. Kennedy^c, W. Raab^d, P. Verhoeve^d, D. Agnolon^d and C. Woffinden^e

^a *The Open University, Walton Hall, Milton Keynes, MK7 6AA, UK*

^b *University of Leicester, Leicester, LE1 7RH, UK*

^c *Mullard Space Science Laboratory, University College London, Surrey, RH5 6NT, UK*

^d *Directorate of Science of the European Space Agency, ESTEC, 2201 AZ, Noordwijk, The Netherlands*

^e *Teledyne-e2v, Chelmsford, Essex, CM1 2QU*

E-mail: matthew.soman@open.ac.uk

ABSTRACT: SMILE, the Solar wind Magnetosphere Ionosphere Link Explorer, is a joint science mission between the European Space Agency and the Chinese Academy of Sciences. The spacecraft will be uniquely equipped to study the interaction between the Earth's magnetosphere-ionosphere system and the solar wind on a global scale. SMILE's instruments will explore this science through imaging of the solar wind charge exchange soft X-ray emission from the dayside magnetosheath, simultaneous imaging of the UV northern aurora and in-situ monitoring of the solar wind and magnetosheath plasma and magnetic field conditions.

The Soft X-ray Imager (SXI) is the instrument being designed to observe X-ray photons emitted by the solar wind charge exchange process at photon energies between 200 eV and 2000 eV. X-rays will be collected using a focal plane array of two custom-designed CCDs, each consisting of 18 μm square pixels in a 4510 by 4510 array.

SMILE will be placed in a highly elliptical polar orbit, passing in and out of the Earth's radiation belts every 48 hours. Radiation damage accumulated in the CCDs during the mission's nominal 3-year lifetime will degrade their performance (such as through decreases in charge transfer efficiency), negatively impacting the instrument's ability to detect low energy X-rays incident on the regions of the CCD image area furthest from the detector outputs. The design of the SMILE-SXI CCDs is presented here, including features and operating methods for mitigating the effects of radiation damage and expected end of life CCD performance. Measurements with a PLATO device that has not been designed for soft X-ray signal levels indicate a temperature-dependent transfer efficiency performance varying between 5×10^{-5} and 9×10^{-4} at expected End of Life for 5.9 keV photons, giving an initial set of measurements from which to extrapolate the performance of the SXI CCDs.

KEYWORDS: X-ray detectors and telescopes; Space instrumentation; Solid State Detectors; X-ray detectors.

* Corresponding author.

Contents

1. Solar wind Magnetosphere Ionosphere Link Explorer (SMILE)	1
1.1 Soft X-ray Imager (SXI)	1
2. The CCD370	3
2.1 Design heritage	3
2.2 CCD optimisation for soft X-ray detection	3
2.3 CCD370 operation for soft X-ray photon counting	5
3. Predicting the performance of the CCD370s	6
3.1 X-rays with On-Chip Pixel Binning	6
3.2 CTI of a PLATO CCD270 with SMILE-like clocking	7
4. Conclusions and further work	8

1. Solar wind Magnetosphere Ionosphere Link Explorer (SMILE)

SMILE, the Solar wind Magnetosphere Ionosphere Link Explorer, is a small class joint venture mission between the European Space Agency and the Chinese Academy of Sciences [1]. With a planned launch date of late 2021, SMILE will be in a unique position to observe the dynamic response of the Earth's magnetosphere to the solar wind impact using an instrument suite made up of the Soft X-ray Imager (SXI), the Ultra-Violet Imager (UVI), and in-situ monitoring provided by a Light Ion Analyser (LIA) and a MAGnetometer (MAG).

The highly elliptical polar orbit will allow SMILE to perform simultaneous observations of soft X-ray emissions from the interaction between the solar wind and the Earth's dayside magnetosheath, and UV excitations in the Northern hemisphere's aurora over a ~48 hour orbital period. SMILE will collect data over a 3-year mission period to further the understanding of how space weather can influence the Earth's magnetosphere and ionosphere.

1.1 Soft X-ray Imager (SXI)

The Soft X-ray Imager (SXI) is one of the primary instruments on SMILE, optimised to photon count over the 200 eV to 2000 eV energy range with a wide field of view (see Table 1). The instrument is designed to image X-rays produced by the process called Solar Wind Charge eXchange (SWCX) [2,3], where photons are emitted from interactions of ions in the solar wind with neutral geocoronal atoms. Earth's SWCX occurs primarily at the boundary of the Earth's magnetopause, and the imager will provide a semi-continuous observation with a time resolution on the order of minutes to monitor its location.

A mechanical drawing of the SXI instrument design is shown in Figure 1. Silicon Micro-Pore Optics (MPOs) arranged in a lobster-eye configuration are used to focus the X-rays onto a focal plane of two large-area Charge-Coupled Devices (CCDs) where the X-rays are directly detected. CCD operation and initial image processing are carried out in the Front End

Electronics (FEE) located under the focal plane, and overall instrument control and collation/compression of the data takes place in the Data Processing Unit (DPU) positioned away from the instrument in the payload module. A large optical baffle is designed to shield the focal plane from stray light (primarily from the Sun and the Earth) and a thermal radiator is used as a passive heat dissipater to reduce the focal plane temperature to below -100 °C. A door in front of the focal plane will be closed as the spacecraft approaches perigee to shield the CCDs from the higher levels of radiation found in the trapped belts.

Table 1. Specifications of the Soft X-ray Imager.

Characteristic	Units	Value
Field of view	degrees	26.5° x 15.5°
Focal length	cm	30
Primary science energy range	eV	200-2000
Instrument mass	kg	~26
Optics mass	kg	<1
Time resolution	minutes	<5

The instrument design (Figure 1) will continue to be optimised and matured up until the instrument Critical Design Review scheduled for February 2019, whilst the CCD design requirements have now been fixed following an iterative performance analysis.



Figure 1. A stripped-down mechanical drawing of the SXI, showing the optics at the top of the instrument that are used to focus the soft X-rays onto the focal plane which is positioned below a shielding door (shown open in this configuration). The CCDs in the focal plane are electrically connected to the Front End Electronics (FEE) that is contained in the blue box. A thermal radiator and optical baffle are not shown here. The instrument interfaces with SMILE’s Payload Module via the tripod design at the base.

2. The CCD370

2.1 Design heritage

The SXI CCDs have been developed to optimise soft X-ray sensitivity throughout the mission lifetime, whilst adopting space-qualified designs and processes from other developments. The CCDs are manufactured by Teledyne-e2v with a design adapted from the PLATO CCD270s [4], so that the qualification of the mechanical and electrical interfaces can be adopted (Figure 2). For example, the silicon carbide packaging, the wire-bonded flex circuitry for the electrical interface, and the package-mounted temperature sensor, will all have been qualified as part of the PLATO programme, so the cost and schedule are reduced for SMILE.

The SXI CCD uses the same electrical interface as the PLATO CCDs, therefore test cameras and procedures for Teledyne-e2v testing can be adopted, and the CCD flight drive electronics can be an adaptation of the PLATO ‘slow camera’ readout electronics, both provided by collaborative partners from UCL’s Mullard Space Science Laboratory.

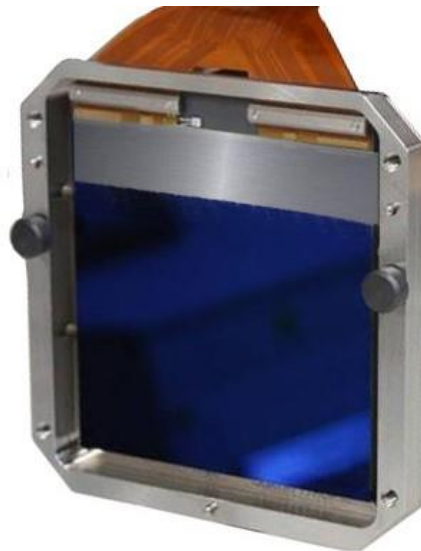


Figure 2. An artist's impression of the SMILE CCD370, with a greyed-out store region across approximately 1/7 of the silicon area. The electrical interface is made through a flex-circuit wire-bonded to the edge of the sensor adjacent to the serial register. A temporary acrylic window is visible in front of the device here, which is part of its travelling and handling jig.

2.2 CCD optimisation for soft X-ray detection

The PLATO CCD270 was designed for the mission's goals of optical imaging with large signal levels. To optimise the device for the SXI application, modifications have been made at the silicon level to maximise the X-ray detection efficiency, at both the beginning and end of operational life. The SMILE SXI CCD is designated as the CCD370. Details of the CCD design and performance are shown in Table 2 and an artist's impression of the device is illustrated in Figure 2.

The detection efficiency for the SXI CCDs is maximised by using back-illuminated and uncoated silicon, with an enhanced passivation process on the back-surface, which has been shown to maximise the quantum efficiency in the soft X-ray range [5].

Table 2. Design parameters of the CCD370 for the Soft X-ray Imager. The split ratio of the image and store areas is subject to change in the final design, but will be approximately 6:1.

Property	Units	Value
Sensitive silicon thickness	μm	16
Native pixel size	$\mu\text{m} \times \mu\text{m}$	18x18
Image area size	pixels	4510 columns x 3791 rows
	mm x mm	81.18 x 68.24
Store area size	pixels	4510 columns x 719 rows
Responsivity	$\mu\text{V electron}^{-1}$	~ 7
Output nodes	-	2
Serial registers	-	1

Throughout the nominal 3 year mission lifetime, the CCDs will experience radiation damage, primarily from trapped and solar protons [6]. The damage from the protons in Earth's radiation belts will be limited by closing the shield door when close to Earth, but loss of performance is still expected in the form of lattice damage to the silicon. Traps formed by lattice damage in the buried channel of the sensor can capture electron(s) whilst the signal is transferred through the detector, and release it at a later time into a different pixel, reducing the efficiency of the transfer of charge through the detector (Charge Transfer Inefficiency, CTI).

At the low end of the primary science energy band, 200 eV X-rays are expected to generate on average approximately 55 electrons. At these low signal levels, degradation in CTI through the mission lifetime can have a significant effect on the number of electrons from an X-ray that are transferred across the ~ 8 cm sensor to be converted to a voltage at the output node. The CTI has been maximised for low signals by including a Supplementary Buried Channel (SBC) in the parallel region of the sensor, and narrowing the channel in the serial register. The SBC takes heritage from Gaia [7], and improves the CTI by reducing the volume of silicon that the small charge packets occupy, therefore minimising the number of traps that the signal electrons encounter [8]. Other methods such as optimised clocking schemes [9] and multi-level clocking will also be considered to maximise performance [10].

To improve the signal to noise ratio at low signal levels, the output amplifier has been modified to increase the responsivity from $\sim 2 \mu\text{V/e}$ to $\sim 7 \mu\text{V/e}$, by adopting a design with heritage in the Euclid CCDs. The high signal handling capacity of the PLATO output is not required, therefore the improved responsivity will allow lower signal levels to be observed above a threshold set by the readout noise.

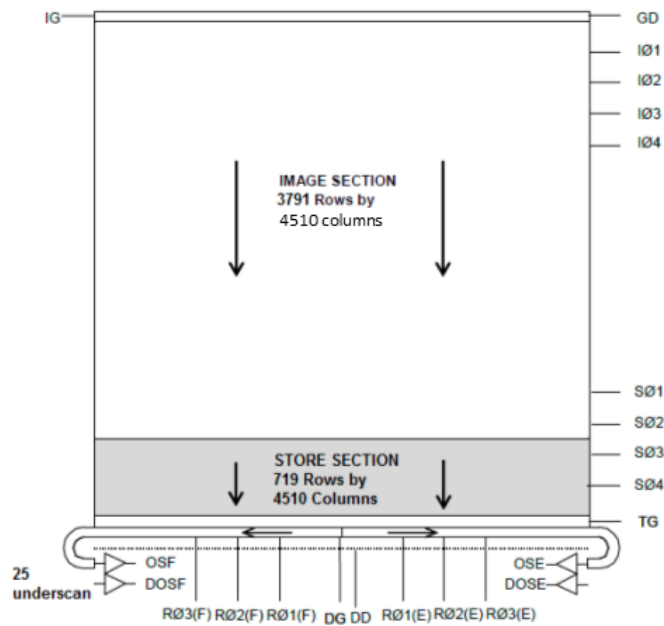


Figure 3. Schematic layout of the SMILE SXI CCD370.

2.3 CCD370 operation for soft X-ray photon counting

Soft X-rays in a 16 μm thick back-illuminated CCD primarily interact in the field-free region at the back surface. Assuming there is no recombination at the back surface, signal electrons are only collected in pixels after they have diffused from their point of generation to the depleted region closer to the front surface. During this process, electrons can move laterally in the CCD and may end up being collected in neighbouring pixels. To recombine signal collected in adjacent pixels for a single X-ray, SXI will operate primarily in a 6×6 binning mode, meaning the majority of X-rays will have their signal recombined in the output node and the signal to noise will be maximised.

The throughput of the SXI CCDs is maximised by using a frame transfer operation allowing an image to be integrated whilst the previous image is being read out. The transfer to exposure time will be maintained at a ratio of greater than 1:10 to minimise any out of time events. In the 6×6 binning mode, the store region can be 1/7 of the total area of the CCD (Figure 3), which improves the usable imaging area relative to the standard 1:1 image to store area ratio. The store section will have separate parallel clocks, and will be mechanically shielded to prevent illumination.

To negate the effects of radiation damage, the CTI can be improved by ensuring that any traps with very slow release times (longer than the integration plus readout time) are filled before signal packets are passed through the trap. This can be achieved by injecting signal as a line in the top of the parallel register, interspersed through the image. The lines of charge injection have been shown to improve the CTI performance (Section 3) but a trade-off is required: image area is lost to the charge injection rows; and signal released from traps originally filled by the charge injection increases the background noise in the rest of the frame. The effect of charge injection on the CTI is discussed in the Section 3.2.

3. Predicting the performance of the CCD370s

To inform the design decisions for the SXI CCD370s, data was collected with a PLATO device, the CCD270-11363-20-01 using a cryostat camera at ESTEC. Part of the image area of one node has been irradiated with 6.5×10^9 protons cm^{-2} (10 MeV equivalent), allowing the performance at approximate SXI Beginning Of Life (BOL) and End Of Life (EOL) levels to be assessed from different regions of the image area (Figure 4). The nominal EOL level for the SXI CCDs is likely to be adjusted from this value as a result of future instrument design optimisation and spacecraft environment modelling, but this irradiation fluence provides a baseline for performance and could be scaled accordingly.

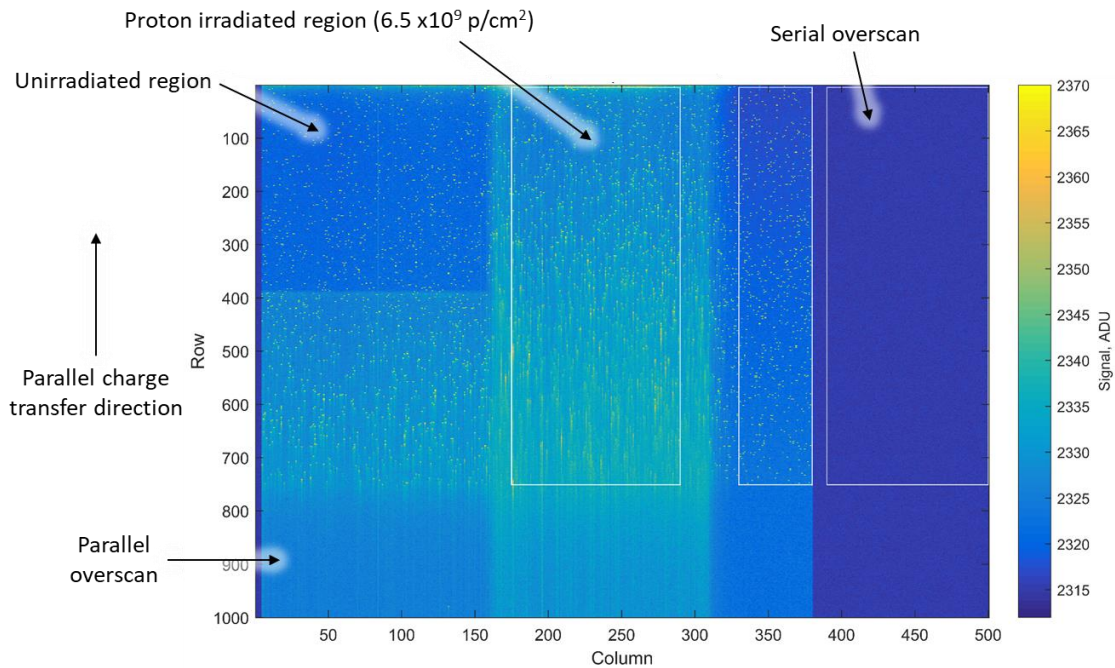


Figure 4. Binned readout from one node of a PLATO CCD270, which has had regions irradiated with protons. This image was recorded with exposure to a ^{55}Fe source, with the detector at 207 K.

3.1 X-rays with On-Chip Pixel Binning

The standard laboratory X-ray source, Iron-55 (^{55}Fe) was used with an exposure time of 0.5 s and resulting flux of approximately 1 X-ray per 3600 native pixels (or 1 X-ray per 100 binned 6×6 pixels). The X-ray events are observed as localised regions of bright pixels in Figure 4. By analysing X-rays observed in the unirradiated section of the detector, the result of pixel binning can be studied.

The pixel output from the average X-ray event is calculated, with the result shown in Figure 5. As expected, more significant charge sharing is observed when no binning is applied. The background noise was calculated to be 5.3 and 5.4 electrons rms for the unbinned and binned cases respectively. A threshold was used, and the number of pixels above this threshold was calculated for each event. The resulting distributions are shown in Figure 5c and Figure 5d, for a threshold of $4.5 \times$ the background noise (chosen to identify pixels which have a signal level clearly above the noise floor). When binning is applied, the majority of these ^{55}Fe (~ 6 keV)

events shift from being 2-pixel events to single pixel events. The 2-pixel events that remain when binned are usually identified as the result of poor CTI in the un-optimised serial clocking pattern used for this initial test. Soft X-rays will have shorter attenuation lengths than those generated by ^{55}Fe , and therefore are more likely to be split across multiple pixels and the benefit of binning will be even more pronounced.

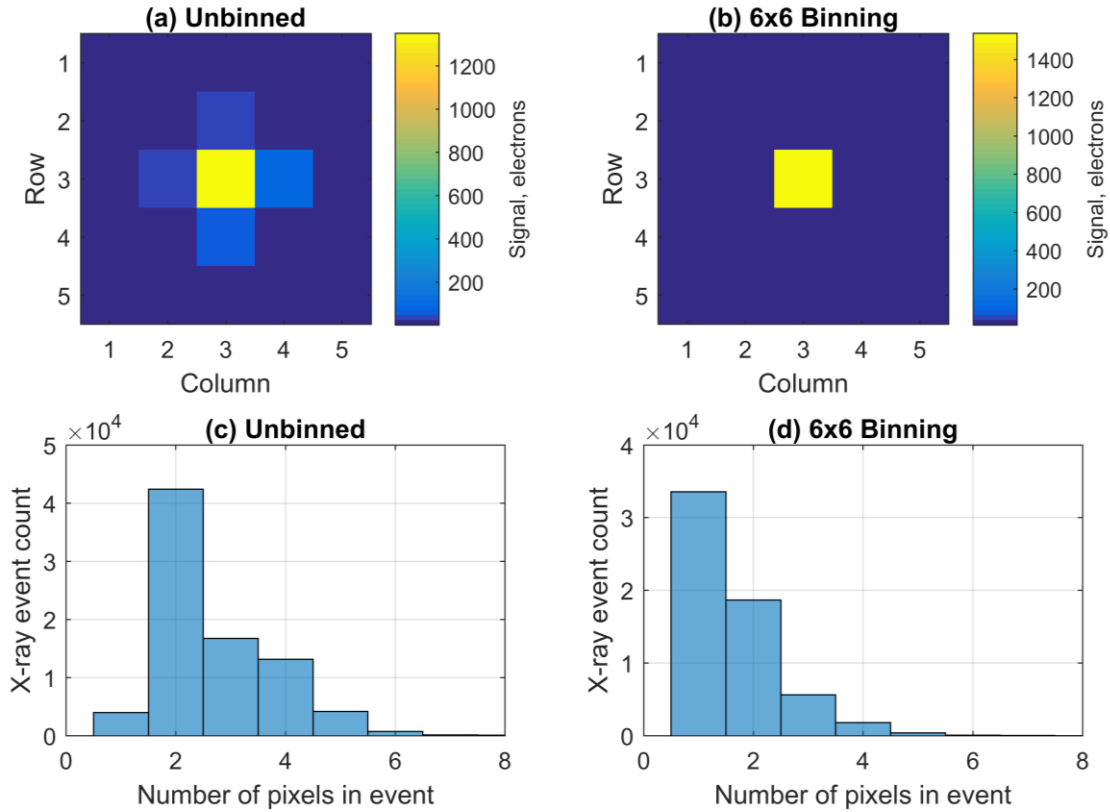


Figure 5. 6×6 pixel binning confines the majority of X-ray events to one or two pixels. The average X-ray event observed in the unirradiated region of interest at 148 K is seen to have signal split into neighbouring pixels when not binned (a), but confined to a single pixel when binned (b). The number of pixels above a threshold ($4.5\times$ the background noise) for each of the binning modes also shows the shift of multi-pixel events when not binning (c) to primarily 1 or 2 pixel events when binning is applied (d).

3.2 CTI of a PLATO CCD270 with SMILE-like clocking

The CTI has also been measured using the ^{55}Fe events observed in the PLATO device. A SMILE-like clocking scheme was devised using a (binned) pixel readout rate of 100 kHz and a line shift time of $22.6\ \mu\text{s}$. The energy of single-pixel X-ray events was studied as a function of row position to determine the average charge loss per transfer, for images recorded at a range of temperatures. Regions of interest selected from the unirradiated and irradiated areas of the detector allowed the performance at the BOL and EOL to be compared.

To investigate the effects of charge injection, lines of approximately 5000 electrons signal level (measured at 163 K) were injected at regular intervals throughout the frame. The parallel CTI as a function of temperature is shown in Figure 6, for three different cases: no charge injection; a

single charge injection line at the beginning of the image; and a charge injection every 450 native pixels (10 per image).

Parallel CTI degrades by ~ 2 orders of magnitude following the approximately EOL equivalent proton irradiation level, and generally the CTI is better at lower temperatures. Charge injection is shown to improve the CTI performance, and essentially delay the onset of CTI degradation to a warmer temperature. Charge injection may therefore be used to negate the loss of CTI performance throughout the mission timeline, or to meet a CTI performance specification at a warmer CCD temperature. Charge injection does result in a loss of usable image area, an increase in image background noise and therefore its use will be a compromise in performance parameters.

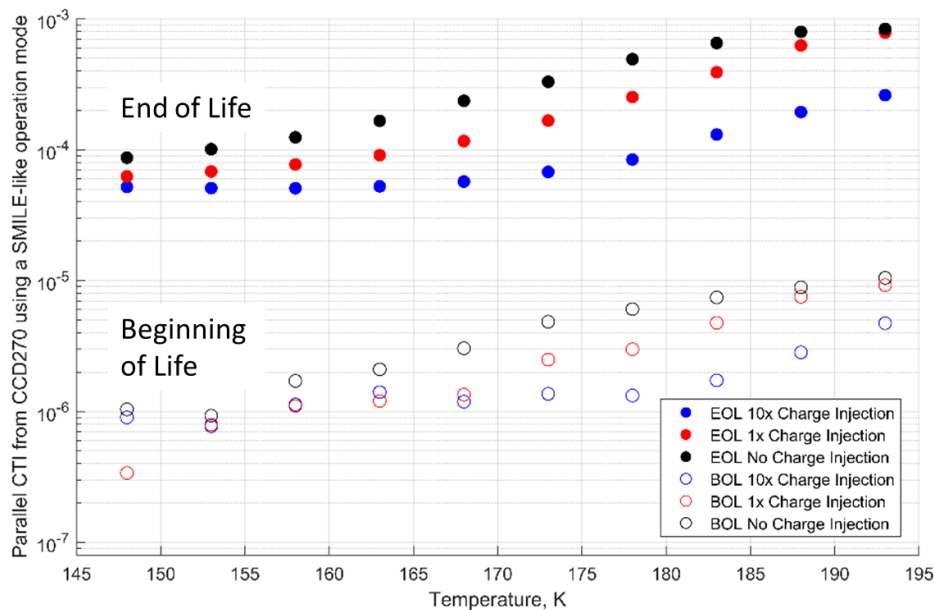


Figure 6. Parallel CTI performance of a PLATO CCD270 operated in SMILE-like conditions (6x6 binning and timing). The parallel CTI is defined as the proportion of signal lost per native pixel transfer.

4. Conclusions and further work

The results presented here, made using a PLATO CCD270 sensor, provide a reference set of measurements from which to predict if the performance of the SMILE CCD370s will be sufficient to meet the science requirements of the mission. However, the prediction must be extrapolated by taking into account many factors including: the X-ray signal levels of interest during the mission are much smaller than the 5.9 keV X-rays measured here; the EOL fluence levels on the SXI CCDs must be more accurately modelled using the latest information about the orbit, spacecraft shielding and radiation environment; the improvements to the device architecture such as the supplementary buried channel in the parallel region are predicted to improve the CTI for small signal level charge packets; the readout clocking scheme of the CCDs will be studied in detail and optimised where possible; and during the mission the CCDs

will be irradiated cold, rather than in room temperature conditions, and therefore the trap landscape may differ. These considerations are being modelled to predict the expected EOL science performance of the SXI CCDs, but the models cannot be verified until measurements are made with the manufactured devices.

The SMILE SXI CCDs have been developed from heritage designs taking elements from PLATO, Gaia and Euclid CCDs. However, the SXI devices (CCD370s) have been optimised for their soft X-ray detection performance with modifications to the back surface treatment, image to store region layout, parallel and serial channels and an increased responsivity output amplifier. Readout with 6×6 native pixel binning will improve the energy resolution and low X-ray energy sensitivity of the detectors, whilst also helping to negate against some poor CTI effects.

The first CCD370s, and their smaller test-device counterparts the CCD380s, are expected to be available for testing in early 2019, and will undergo both radiation damage testing and calibration with soft X-ray sources. Readout timing and operation schemes will be optimised for maximising the soft X-ray sensitivity across the entire image up to and beyond the EOL. After launch in 2021, the SMILE spacecraft will allow scientists across the ESA-CAS collaboration to monitor the magnetosphere's dynamic response to the solar wind and further our understanding of how space weather contributes to the workings of our solar system.

Acknowledgments

The authors would like to thank staff of the Payload Technology Validation section (Future Missions Office at ESA's Directorate of Science) for enabling and performing the measurements and proving the test data into this study for the SMILE programme.

References

- [1] W. Raab et al., *SMILE: A joint ESA/CAS mission to investigate the interaction between the solar wind and Earth's magnetosphere*, Proc. SPIE 9905, Space Telescopes and Instrumentation 2016: Ultraviolet to Gamma Ray, **990502** (2016). doi:10.1117/12.2231984.
- [2] K. Dennerl et al., *Solar system X-rays from charge exchange processes*, *Astronomische Nachrichten* **333** (2012) 324. doi:10.1002/asna.201211663.
- [3] B. Walsh et al., *Wide field-of-view soft X-ray imaging for solar wind magnetosphere interactions*, *Journal of Geophysical Research*, **121** (2016) 3353-3361
- [4] J. Endicott, et al., *Charge-coupled devices for the ESA PLATO M-class Mission*, Proc. of SPIE **8453** (2012).
- [5] I. Moody et al., *CCD QE in the Soft X-ray Range*, Teledyne-e2v White Paper (14 March 2017).
- [6] A. Holland et al., *Techniques for minimizing space proton damage in scientific charge coupled devices*, *IEEE Transactions on Nuclear Science* **38** (1991) 1663.

- [7] G. M. Seabroke, et al., *Digging supplementary buried channels: investigating the notch architecture within the CCD pixels on ESA's Gaia satellite*, Monthly Notices of the Royal Astronomical Society **430.4** (2013) 3155-3170.
- [8] A. Clarke, et al., *Modelling charge storage in Euclid CCD structures*, JINST **7** (2012) C01058.
- [9] D. J. Hall, et al., *Optimisation of device clocking schemes to minimise the effects of radiation damage in charge-coupled devices*, IEEE Transactions on Electron Devices **59** (2012) 1099.
- [10] N. J. Murray, et al., *Multi-level parallel clocking of CCDs for: improving charge transfer efficiency, clearing persistence, clocked anti-blooming, and generating low-noise backgrounds for pumping*, Proc. SPIE 8860, UV/Optical/IR Space Telescopes and Instruments: Innovative Technologies and Concepts VI, **886020** (2013).